Pergamon

PII: S0277-5387(97)00497-X

Polyhedron Vol. 17, No. 7, pp. 1183–1193, 1998

0277-5387/98 $19.00+0.00

Synthesis of 2,6-bis(diphenylphosphinomethyl) pyridine-monoligand-rhodium(I) complexes [Rh(PNP)L]X with L = pyridine, CH_3CN, DMSO and X = CF_3SO_3, BF_4 from the corresponding ethylene complex and comparison of the structures to the piperidine complex (L = piperidine, X = BF_4)†

Christine Hahn,[a] Joachim Sieler[b] and Rudolf Taube[c]*

[a] Universität Würzburg, Institut für Anorganische Chemie, Am Hubland, D-97074 Würzburg, Germany

[b] Universität Leipzig, Institut für Anorganische Chemie, Linnéstr. 3, D-04103 Leipzig, Germany

[c] Technische Universität München, Anorganisch-Chemisches Institut, Lichtenbergstrae 4, D-85747 Garching, Germany

(Received 13 August 1997; accepted 26 November 1997)

Abstract—Investigation of the coordination conditions at the 2,6-bis(diphenylphosphinomethyl)pyridine-rhodium(I) fragment $[Rh(PNP)]^+$ by X-ray crystallography showed a square planar geometry of the neutral chloro and the cationic piperidine complexes, [Rh(PNP)Cl] (**1**) and $[Rh(PNP)(pip)]BF_4$ (**2**). New cationic rhodium(I) complexes [Rh(PNP)L]X (L = pyridine, X = SO_3CF_3 **3**; L = CH_3CN, X = SO_3CF_3 **4a**, X = BF_4 **4b**; L = DMSO, X = SO_3CF_3 **5**) have been synthesized from the ethylene complexes $[Rh(PNP)(C_2H_4)]X$ by substitution of the ethylene by the ligand L (L = py, CH_3CN, or DMSO). The complexes **3–5** were characterized by IR spectroscopy, ^1H-, ^{13}C-, and ^{31}P-NMR spectroscopy and X-ray crystallography. The influence of the ligands on the structure of the complexes was investigated. The *cis* influence was determined by measurement of the coupling constant J_{P-Rh} and the average length of the Rh—P bonds and the *trans* influence by the length of the Rh—N(1) bond. © 1998 Elsevier Science Ltd. All rights reserved.

Keywords: cationic rhodium(I) complexes; 2,6-bis(diphenylphosphinomethyl)pyridine; X-ray crystal structure analyses; ethylene substitution; *cis* and *trans* influence.

The hydroamination of olefins, that is the N–H addition at the C–C double bond represents the simplest amine synthesis. It is especially interesting from the point of view of atom economy, since no by-product is formed (cf. eqn (1)). Although during the last decades several catalytic routes have been discovered using structurally different catalysts, until now no convenient catalyst for the hydroamination of olefins is known [1].

We have found that the cationic ethylene rhodium(I) complex $[Rh(C_2H_4)(PPh_3)_2(Me_2CO)]PF_6$, is the first complex which catalyzes the addition of secondary amines such as piperidine to the ethylene at

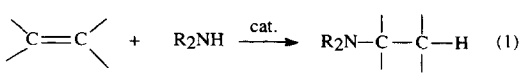

(1)

† Dedicated to Prof. Dr W. A. Herrmann on the occasion of his 50th birthday.

* Author to whom correspondence should be addressed.

room temperature and under normal pressure [2,3], but only a low productivity is reached.

Using the tridentate ligand 2,6-bis(diphenylphosphinomethyl)pyridine (PNP) [4] cationic olefin rhodium(I) complexes [Rh(PNP)(olefin)]X (olefin = ethylene, styrene; X = BF_4, PF_6, CF_3SO_3) have been synthesized and characterized as model compounds for the catalyst complex [5]. The corresponding amine complexes [Rh(PNP)(HNR_2)]X (HNR_2 = piperidine, $HNMe_2$, $HNEt_2$) were obtained from the olefin complexes and secondary amines by substitution of the olefin without attack at the C–C double bond [5]. These Rh(PNP) complexes have been used as models to study the course and mechanism of the catalytic reaction.

In this paper we present the X-ray structure analyses of the neutral chloro-complex [Rh(PNP)Cl] [6] and the cationic piperidine complex [Rh(PNP)(pip)]BF_4 [5], report the synthesis and characterization of further monoligand complexes [Rh(PNP)L]X, and give a comparison of the structure of Rh(PNP) complexes as they change with the ligand variation.

EXPERIMENTAL

General

All reactions were carried out under dry argon. Ethanol, acetone and acetone-d_6 were refluxed over 4 Å molecular sieves and degassed by bubbling argon. Toluene, THF and diethyl ether were refluxed over Na/benzophenone and toluene-d_8 over K/Na alloy. Pyridine, acetonitrile and DMSO were dried over 4 Å molecular sieves and distilled before use.

Infrared spectra were recorded in nujol ([Rh(PNP)Cl] **1**) or as KBr pellets (cationic complexes **2**–**5**) on a Perkin-Elmer FT-IR 16 spectrometer. The ^{1}H-, ^{13}C-{^{1}H}, and ^{31}P{^{1}H}-NMR spectra were recorded at 300, 75, and 121 MHz respectively, on a Varian Gemini 300 NMR spectrometer. The ^{1}H- and ^{13}C-NMR shifts were referenced to the resonance of the residual protons of the solvents. The ^{31}P-NMR shifts were referenced to an external reference of 85% H_3PO_4. Elemental analyses of C, H and N were carried out on a LECO CHN 932 analyzer and Rh was determined using a photometric method [7].

The complex [{RhCl(COT)$_2$}$_2$] (COT = cyclooctene) was prepared according to the procedure in [8].

Synthesis of [Rh(PNP)Cl] (**1**)

The procedure described in [6] was slightly modified: A solution of 4.1 g (8.6 mmol) of 2,6-bis(diphenylphosphinomethyl)pyridine in 200 ml of toluene was added dropwise to a solution of 3.1 g (8.6 mmol) of [{RhCl(COT)$_2$}$_2$] in 200 ml of toluene over 5 hours. The resulting suspension was stirred overnight. The mixture of yellow and red solids which precipitated was filtered off and washed with 30 ml of ethanol to obtain the crude red product. Another fraction was obtained crystallized by concentration of the mother liquor (toluene solution) to 30 ml under reduced pressure. Both fractions were collected and recrystallized from refluxing toluene.

Yield: 2.6 g (4.3 mmol, 50%). M.p.: 230°C. ^{31}P-NMR δ (ppm) in toluene-d_8: 21.4, ($J_{P\text{-}Rh}$ = 152 Hz).

Synthesis of [Rh(PNP)(pip)]BF_4 (**2**)

The complex **2** was obtained from the reaction of [Rh(PNP)(C_2H_4)]BF_4 with an excess of piperidine according to the procedure in [5].

Synthesis of [Rh(PNP)[(py)]SO_3CF_3 (**3**)

1 ml (12 mmol) of pyridine was added to a suspension of 926 mg (1.2 mmol) of [Rh(PNP)(C_2H_4)]-SO_3CF_3 [5] in 15 ml of THF. The solid dissolved with evolution of gas and the solution changed in colour to orange. After stirring for 1 h the reaction mixture was filtered and the crude product was precipitated by dropwise addition diethyl ether to the filtrate. The orange-yellow solid was collected by filtration, washed with diethyl ether and dried in vacuum. The crude product was recrystallized from refluxing THF.

Yield: 716 mg (0.89 mmol, 74%). M.p.: 191°C. Found: C, 55.31; H, 3.80; N, 3.64; Rh 13.07. Calc. for $C_{37}H_{32}F_3N_2O_3P_2RhS$: C, 55.10; H, 3.99; N, 3.47; Rh, 12.76%. IR ν (cm^{-1}): 1604, 1564 (py); 1266, 1224, 1154, 1030, 638, 572 (CF_3SO_3). ^{1}H-NMR: δ (ppm): 4.36 (vt, N = 4.4 Hz, 4H, CH_2P), 7.15 (t, $J_{H\text{-}H}$ = 7.5 Hz, 2H, py), 7.49–7.38 (m, 14H, py[PNP], Ph), 7.65–7.60 (m, 9H, py[PNP], Ph), 7.74 (t, $J_{H\text{-}H}$ = 7.9 Hz, 1H, py), 8.75 (d, $J_{H\text{-}H}$ = 5.0 Hz, 2H, py). ^{13}C-NMR: δ (ppm): 43.6 (vt, N = 12.7 Hz, CH_2P), 122.7 (vt, N = 5.8 Hz, 3,5-py[PNP]), 126.0 (s, 3,5-py), 129.8 (vt, N = 4.8 Hz, PC_{meta}), 131.3 (s, PC_{para}), 133.3 (vt, N = 7.2 Hz, PC_{ortho}), 137.3 (s, 4-py[PNP]), 137.4 (s, 4-py), 155.3 (s, 2-py), 163.8 (vt, N < 3 Hz, 2,6-py[PNP]).

Syntheses of [Rh(PNP)(CH_3CN)]X (X = SO_3CF_3 **4a**, X = BF_4 **4b**) *and* [Rh(PNP)(DMSO)]SO_3CF_3 (**5**)

The complex **4a** was prepared from the reaction of 862 mg (1.14 mmol) of [Rh(PNP)(C_2H_4)]SO_3CF_3 and 5 ml of acetonitrile and complex **4b** from 693.3 mg (1.00 mmol) of [Rh(PNP)(C_2H_4)]BF_4 and 5 ml of acetonitrile in 15 ml of THF respectively. The complex **5** was prepared from 805 mg (1.06 mmol) of [Rh(PNP)(C_2H_4)]SO_3CF_3 and 1 ml of DMSO in 15 ml of THF. The complexes **4a**, **4b** and **5** were isolated in the same manner described for the complex **3**, except that the crude products precipitated as oils upon dropwise addition of diethyl ether to the reaction solution.

The oils crystallized after several hours. The crude products were recrystallized from refluxing THF.

4a: Yellow-brown crystalline solid, yield: 779 mg (0.89 mmol, 78%). M.p.: 126–130°C. Found: C, 52.92; H, 3.89: N, 4.04; Rh, 13.04. Calc. for $C_{34}H_{30}F_3N_2O_3P_2RhS$: C, 53.14; H, 4.21; N, 3.64; Rh, 13.39%. IR ν (cm^{-1}): 1602, 1566, (py); 1268, 1224, 1154, 1030, 638, 572 (CF_3SO_3); 2279, 2325 (CH_3CN). ^{1}H-NMR δ (ppm): 4.29 (vt, N = 4.4 Hz, 4H, CH_2P), 2.40 (s, 3H, CH_3), 7.53 (m, 14H, py, Ph), 7.79 (t, J_{H-H} = 7.9 Hz, 1H, py), 7.89–7.86 (m, 8H, Ph). ^{13}C-NMR δ (ppm): 3.8 (s, CH_3), 42.9 (vt, N = 11.6 Hz, CH_2P), 122.8 (vt, N = 5.1 Hz, 3,5-py), 129.9 (vt, N = 5.1 Hz, PC_{meta}), 131.5 (s, PC_{para}), 133.5 (vt, N = 7.3 Hz, PC_{ortho}), 138.0 (s, 4-py), 164.0 (vt, N < 3 Hz, 2,6-py).

4b: Yellow-brown crystalline solid, yield: 572 mg (0.81 mmol, 81%). IR ν (cm^{-1}): 1596, 1562 (py): 1268, 1062, (BF_4); 2283, 2330 (CH_3CN). ^{1}H-NMR δ (ppm): 2.41 (s, 3H, CH_3), 4.33 (vt, N = 4.4 Hz, 4H, CH_2P), 7.53 (m, 14H, py, Ph), 7.81 (t, J_{H-H} = 7.9 Hz, 1H, py), 7.86–7.90 (m, 8H, Ph). ^{13}C-NMR δ (ppm): 3.4 (s, CH_3), 42.5 (vt, N = 11.6 Hz, CH_2P), 122.5 (vt, N = 5.1 Hz, 3,5-py), 129.6 (vt, N = 5.1 Hz, PC_{meta}), 131.3 (s, PC_{para}), 133.3 (vt, N = 7.3 Hz, PC_{ortho}), 137.8 (s, 4-py), 163.8 (vt, N < 3 Hz, 2,6-py).

5: Yellow crystalline solid, yield: 763 mg (0.97 mmol, 91%). M.p.: 138–142°C. Found: C, 51.57; H, 4.34: N, 2.05; Rh, 12.18. Calc. for $C_{34}H_{33}F_3NO_4P_2RhS_2 \cdot 1/2\ (CH_3)_2CO$: C, 51.37; H, 4.43; N. 1.66; Rh, 12.22%. IR ν (cm^{-1}): 1600, 1562, (py); 1272, 1224, 1162, 1028, 636, 572 (CF_3SO_3); 1100 (DMSO). ^{1}H-NMR δ (ppm): 2.68 (s, 6H, CH_3), 4.51 (vt, N = 4.4 Hz, 4H, CH_2P), 7.59–7.54 (m, 14H, py, Ph), 7.86 (t, J_{H-H} = 7.8 Hz, 1H, py), 7.99–7.94 (m, 8H, Ph). ^{13}C-NMR δ (ppm): 44.2 (vt, N = 12.4 Hz, CH_2P), 50.6 (s, CH_3), 123.1 (vt, N = 5.3 Hz, 3,5-py), 130.1 (vt, N = 5.0 Hz, PC_{meta}), 132.2 (s, PC_{para}), 134.3 (vt, N = 6.8 Hz, PC_{ortho}), 140.5 (s, 4-py), 162.8 (vt, N < 3 Hz, 2,6-py).

X-ray structural analyses

A data collection and structure determination summary for the compounds **1–5** is given in Table 1. An empirical absorption correction for **1** and **5** (Ψ-scan, 10 reflections) and **2**, **3** and **4b** (SADABAS [9]) was applied. The structures were solved by Patterson methods and refined with a full matrix least-squares algorithm using the programs SHELXS-86 [10] and SHELXL-93 [11], respectively. Anisotropic displacement parameters for all nonhydrogen atoms were used. For compounds **1** and **5** the hydrogen atoms were placed in calculated positions and refined isotropically. The hydrogen atoms for the compounds **2**, **3** and **4b** could be located in difference Fourier syntheses and were included in the final cyclus of the refinement with isotropic displacement parameters. The numbering of the atoms for the 2,6-bis (diphenylphosphinomethyl)pyridine-rhodium(I) fragment $[Rh(PNP)]^+$ is the same for compounds **1–5**.

Further details of the crystal structure determination are deposited at the Fachinformationszentrum Karlsruhe, D-76344 Leopoldshafen-Eggenstein, and may be obtained by quoting the depository numbers CSD 407975 (**1**), CSD 407974 (**2**), CSD 407973 (**3**), CSD 407972 (**4b**), CSD 407971 (**5**).

RESULTS AND DISCUSSION

X-ray structure analysis of [Rh(PNP)Cl] (**1**) *and* $[Rh(PNP)(pip)]BF_4$ (**2**)

The structure of the chloro-PNP-rhodium(I) complex [Rh(PNP)Cl] (**1**) [6] represents the origin for further ligand variation at the $[Rh(PNP)]^+$ fragment. Therefore the characterization of **1** by X-ray crystallography is a contribution of fundamental importance for our model studies.

The chloro-complex **1** was prepared according to the literature procedure [6], except that toluene was used as a solvent. When the PNP ligand solution was added dropwise to the solution of $[\{RhCl(COT)_2\}_2]$ the yellow dinuclear complex $[Rh_2(PNP)_3]Cl_2$ as well as the red chloro-complex precipitated. The dinuclear complex could be separated by extraction of the mixture with ethanol, leaving the red chloro-complex **1** as a solid. Further concentration of the mother liquor (toluene solution) gave a further preciptate of **1**, from which X-ray quality single crystals could also be obtained. The melting point of 230°C and the characteristic IR bands for the pyridine ring vibrations at 1550 and 1586 cm^{-1} of **1** are in good agreement with the literature data [6]. In the ^{31}P-NMR spectrum a doublet appears at 21.4 ppm ($J_{P\ Rh}$ = 152 Hz). The molecular structure of the chloro-complex is shown in Fig. 1. The PNP ligand atoms and Cl are coordinated to the rhodium atom in a nearly square planar geometry. The N(1)–Rh–Cl(1) angle (178.10(12)°) is not significantly distorted from the linearity whereas the P(1)–Rh–P(2) (163.53(5)°) is relatively small due to the steric constraints of two five-membered rings formed by coordination of the PNP ligand at the rhodium atom. The Rh–Cl(1) distance (2.344(2) Å) is significantly shorter than that found, for example, in $[RhCl(PPh_3)_3]$ (red allotrope, 2.376(4) Å) [12].

As reported in [5], the X-ray crystal structure analysis of the cationic olefin complexes [Rh(PNP)(olefin)]BF_4 show a square planar coordination geometry of the complex cation without any close interaction of the Rh with the BF_4^- ion. The related piperidine complex $[Rh(PNP)(pip)]BF_4$ **2**, obtained from the reaction of the ethylene complex $[Rh(PNP)(C_2H_4)]BF_4$ with an excess of piperidine [5] is also without coordination interaction between the central atom and the anion. Single crystals suitable for X-ray crystal structure analysis were obtained from a solution of **2** in acetone overlayered with diethyl ether. The molecular structure of the complex cation of **2** is shown in Fig. 2. The Rh–N(2) distance (2.122(3)Å) is

Table 1. Crystallographic data and parameters of X—ray data collection and refinement

Compound	**1**	**2**	**3**	**4b**	**5**
Formula	$C_{31}H_{27}ClNP_2Ph$	$C_{36}H_{38}BF_4N_2P_2Rh \cdot 0.5CH_3OCH_3$	$C_{37}H_{32}F_3N_2O_3P_2RhS$	$C_{36}H_{36}BF_4N_2OP_2Rh$	$C_{34}H_{33}F_3NO_4P_2RhS_2 \cdot 0.5\ CH_3COCH_3$
Formula weight [g · mol^{-1}]	613.84	766.34	806.56	764.33	834.62
Crystal	Prism ; red	Prism ; yellow	Needles ; orange	Prism ; yellow	Needles ; yellow
Crystal size [mm]	0.28 × 0.26 × 0.22	0.24 × 0.22 × 0.20	0.32 × 0.26 × 0.22	0.22 × 0.18 × 0.18	0.32 × 0.15 × 0.12
Crystal system	Monoclinic	Monoclinic	Monoclinic	Monoclinic	Monoclinic
Space group ; Z	$P2_1/c$; 4	$C2/c$	$P2_1/c$	$C2/c$	$C2/c$
a [Å]	10.431(2)	18.2124(11)	11.040(2)	17.0796(9)	30.749(5)
b [Å]	15.767(5)	14.9278(9)	17.239(3)	15.0508(8)	11.0650(10)
c [Å]	17.210(1)	26.136(2)	18.250(4)	27.450(2)	21.653(2)
α [°]	90.0(0)	90.0(0)	90.0(0)	90.0(0)	90.0(0)
β [°]	104.18(3)	96.8760(10)	97.40(3)	97.2270(10)	100.280(10)
γ [°]	90.0(0)	90.0(0)	90.0(0)	90.0(0)	90.0(0)
Volume [Å^3]	2744(2)	7054.5(7)	3444.4(12)	7000.4(6)	7249(2)
Density (calc.) [Mg · m^{-3}]	1.486	1.443	1.555	1.450	1.530
Absorption coeff. [mm^{-1}]	0.857	0.627	0.706	0.632	0.731
Diffractometer	STADI4 (Stoe)	CCD-System (Siemens)	CCD-System (Siemens)	CCD-System (Siemens)	STADI4 (Stoe)
θ range [°]	1.78–27.00	1.57–23.24	1.63–23.26	1.50–26.18	1.91–25.01
Reflections/R_{int}	5975/0.072	5009/0.0281	4916/0.0483	6170/0.0242	6393/0.0143
Data/parameters	5294/347	5009/558	4916/570	6170/16/527	6393/446
Goof on F^{f2}	0.984	1.190	1.132	0.774	1.038
R_1/wR_2 [$I > 2\sigma(I)$]	0.0386/0.0962	0.0356/0.1012	0.0437/0.1006	0.0356/0.0851	0.0336/0.0842
R_1/wR_2 [all data]	0.1125/0.1212	0.0412/0.1036	0.0542/0.1066	0.0443/0.0924	0.0440/0.0917
Largest diff. peak [e · $^{-3}$]	0.965	1.344	0.403	0.512	1.268

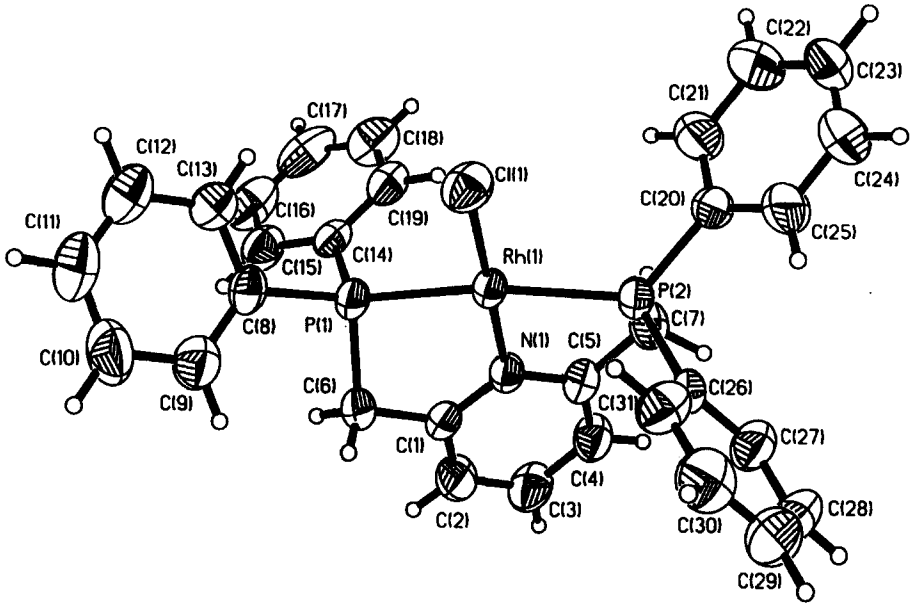

Fig. 1. ORTEP drawing structure of [Rh(PNP)Cl] **1**. Selected bond lengths [Å] and angles [°]: Rh—N(1) 2.040(4), Rh—Cl(1) 2.344(2), Rh—P(1) 2.263(2), Rh—P(2) 2.260(2), P(1)—C(6) 1.833(5), P(2)—C(1) 1.847(7), P(1)—Rh—P(2) 163.53(5), N(1)—Rh—P(1) 81.67(12), N(1)—Rh—P(2) 82.20(12), N(1)—Rh—Cl(1) 178.10(12).

comparable to those found in $[RhCl(C_2H_4)(pip)_2]$ (A form, 2.085(3) and 2.220(3) Å) [13].

Synthesis and characterization of [Rh(PNP)L]X (L = py, X = SO_3CF_3 **3**; L = CH_3CN, X = SO_3CF_3 **4a**, X = BF_4 **4b**)

To investigate the variation of the *N*-bonding conditions ($Nsp^3 \rightarrow Nsp^2 \rightarrow Nsp$) at the $[Rh(PNP)]^+$ fragment the pyridine and acetonitrile complexes [Rh(PNP)L]X (L = py, X = SO_3CF_3 **3**; L = CH_3CN, X = SO_3CF_3 **4a**, X = BF_4 **4b**) were synthesized. The complexes $[Rh(PNP)(C_2H_4)]X$ (X = SO_3CF_3, BF_4) were used as starting compounds since they are easily accessible [5]. When an excess of the respective ligand L was added to a suspension of the ethylene complex in THF at room temperature it reacted immediately by displacement of ethylene, cf. eqn. (2).

The complexes **3**, **4a** and **4b** were obtained in good yields as crystalline solids which are stable in air and are soluble in acetone, THF, and ethanol and insoluble in diethyl ether and hydrocarbons such as toluene or hexane. In the IR spectrum of **3**, **4a** and **4b** the bands observed at about $\nu = 1603$ cm^{-1} and 1565 cm^{-1} indicate coordination of the pyridine ring of the tridentate PNP-ligand [4]. The different absorption bands for the $CF_3SO_3^-$ anion (see Experimental section) found in the spectra of the complexes **3** and **4a** as well the band at 1062 cm^{-1} found for the BF_4^- anion, suggest that these anions are not coordinated to rhodium [14,15], as was also found for the ethylene and piperidine complexes [Rh(PNP)L]X (L = C_2H_4, piperidine; X = SO_3CF_3, BF_4) [5]. The complexes **4a** and **4b** show the characteristic bands of coordinated acetonitrile at about 2280 and 2330 cm^{-1} [16].

The complexes **3**, **4a** and **4b** were further characterized by ^{31}P-, ^1H-, and ^{13}C-NMR spectroscopy. In

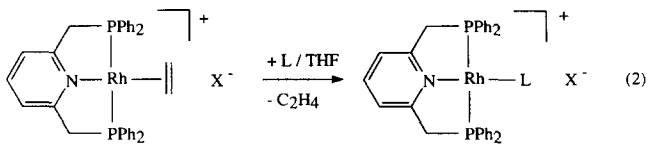

(2)

L = pyridine, X = CF_3SO_3 **3**
L = CH_3CN, X = CF_3SO_3 **4a**
X = BF_4 **4b**

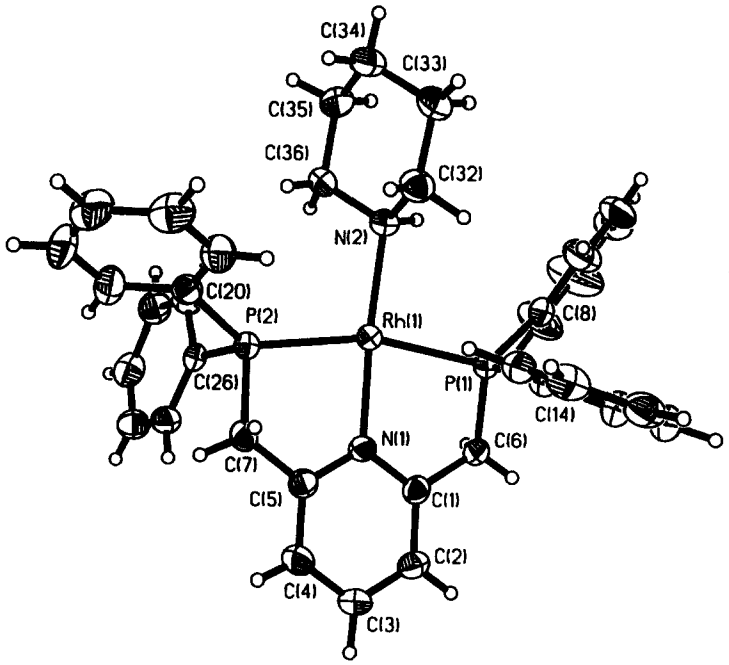

Fig. 2. ORTEP drawing structure of the cation of $[Rh(PNP)(pip)]BF_4$ **2**. Selected bond lengths [Å] and angles [°]: Rh—N(1) 2.062(3), Rh—N(2) 2.122(3), Rh—P(1) 2.2512(10), Rh—P(2) 2.3051(10), P(1)—C(6) 1.837(4), P(2)—C(7) 1.835(4), P(1)—Rh—P(2) 163.43(4), N(1)—Rh—P(1) 81.25(9), N(1)—Rh—P(2) 82.33(9), N(1)—Rh—N(2) 175.57(12), C(32)—N(2)—Rh 112.6(3), C(36)—N(2)—Rh 116.4(2).

the ^{31}P-NMR spectrum a doublet was found at 30.9 ppm ($J_{P\text{-}Rh}$ = 152 Hz) for **3**, 31.7 ppm ($J_{P\text{-}Rh}$ = 142 Hz) for **4a** and 30.6 ppm ($J_{P\text{-}Rh}$ = 143 Hz) for **4b**. The ^{1}H- and ^{13}C-NMR chemical shifts of the coordinated ligands (pyridine, acetonitrile) were shifted down field in comparison to the free ligand, as presented in Table 2.

Suitable single crystals of the pyridine complex **3** were obtained from a solution of the complex in acetone overlayered with diethyl ether while single crystals of **4b** were obtained from a concentrated solution of **4b** in acetone. The molecular structures of the complex cations $[Rh(PNP)(py)]^+$ and $[Rh(PNP)(CH_3CN)]^+$ are shown in Figs 3 and 4, respectively. Both exhibit a square planar coordination geometry. The X-ray crystal structure analyses of **3** and **4b** confirms the non-coordination of the $CF_3SO_3^-$ as well as the BF_4^- ions. The pyridine ligand in the complex **3** is nearly perpendicularly orientated to the coordination plane. An almost linear arrangement of Rh–N(2)–C(33)–C(32) is generated by the end-on coordination of the acetonitrile in the complex **4b** (C(33)–N(2)–Rh 173.7(3)°, N(2)–C(33)–C(32) 177.1(5)°) similar to that found for the structurally related cationic acetonitrile complex $[Rh(PPh_3)_3(CH_3CN)]BF_4$ (C–N–Rh 169.5(11)°, N–C–C 177.2(14)°) [17].

Table 2. ^{1}H- and ^{13}C-NMR chemical shifts of the free and coordinated ligands L (pyridine, acetonitrile) in **3** and **4a**

	^{1}H-NMR		^{13}C-NMR	
Ligand	Free	Coordn	Free	Coordn
Pyridine (**3**)	8.62, 7.69, 7.29	8.75, 7.74, 7.15	149.9, 136.2, 124.2	155.3, 137.4, 126.0
CH_3CN (**4a**)	1.93	2.40	118.2, 1.3	130.7 ($J_{C\text{-}Rh}$ = 11.4 Hz), 3.8

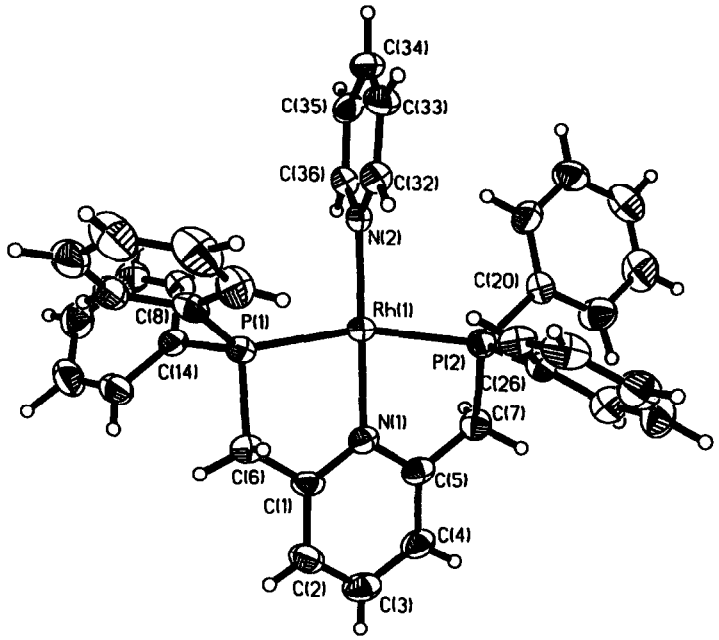

Fig. 3. ORTEP drawing structure of the cation of $[Rh(PNP)(py)]SO_3CF_3$ **3**. Selected bond lengths [Å] and angles [°]: Rh—N(1) 2.068(4), Rh—N(2) 2.063(4), Rh—P(1) 2.2705(12), Rh—P(2) 2.2819(13), P(1)—C(6) 1.835(5), P(2)—C(7) 1.836(5), P(1)—Rh—P(2) 163.06(4), N(1)—Rh—P(1) 83.12(10), N(1)—Rh—P(2) 81.20(10), N(1)—Rh—N(2) 177.37(14), C(32)—N(2)—Rh 122.9(3), C(36)—N(2)—Rh 120.3(3).

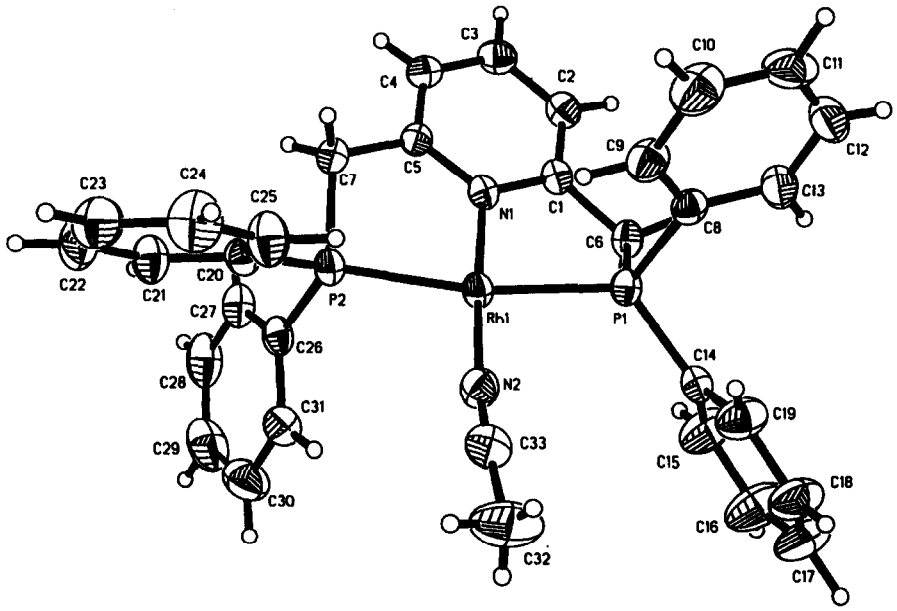

Fig. 4. ORTEP drawing structure of the cation of $[Rh(PNP)(CH_3CN)]BF_4$ **4b**. Selected bond lengths [Å] and angles [°]: Rh—N(1) 2.045(3), Rh—N(2) 1.984(3), Rh—P(1) 2.2648(8), Rh—P(2) 2.2770(8), P(1)—C(6) 1.828(3), P(2)—C(7) 1.838(4), P(1)—Rh—P(2) 166.34(4), N(1)—Rh—P(1) 82.82(7), N(1)—Rh—P(2) 83.54(7), N(1)—Rh—N(2) 175.53(14), C(33)—N(2)—Rh 173.7(3), N(2)—C(33)—C(32) 177.1(5).

Comparing the Rh–N(2) distances in the *N*-donor ligand complexes [Rh(PNP)L]X (L = piperidine, pyridine, acetonitrile) a significant shortening of this bond length is observed according to the hybridization of the nitrogen atom ($Nsp^3 \rightarrow Nsp^2 \rightarrow Nsp$): 2.122(3) for **2**, 2.063(4) for **3** and 1.984(3) for **4b**.

Attempts at the preparation of O-donor ligand complexes

In a manner analogous to the synthesis of the *N*-donor complexes **2–4**, attempts were made to prepare complexes with strong *O*-donor ligands such as HMPT, DMSO and DMF from the ethylene complex $[Rh(PNP)(C_2H_4)]SO_3CF_3$. However, the ethylene could not be substituted by HMPT and DMF. Even after refluxing of the ethylene complex with an excess of HMPT or DMF in THF over several hours, only the starting complex could be isolated. Also acetone and THF both showed no tendency to coordinate. This is in contrast to the coordination of *O*-donor ligands to the rhodium(I) in the complexes $[Rh(C_2H_4)_2(solv)_2]^+$ (solv = THF, acetone) [18] or in the catalyst complex $[Rh(C_2H_4)(PPh_3)_2(Me_2CO)]PF_6$. This indicates the weak affinity of the rhodium(I) in the PNP-complex toward *O*-donor ligands, which are not able to compete with the coordinated ethylene. With HMPT the coordination may be additionally suppressed by steric hindrance as similarly observed for the sterically comparable di-*iso*-propylamine which also did not react with the ethylene complex [5].

DMSO, however, reacts immediately when it is added dropwise to a suspension of the ethylene complex in THF at room temperature. The reaction solution changed in colour to yellow and the evolution of gas was observed. However, the isolated complex proved to be an *S*-donor ligand complex (cf. eqn (3)) as shown by IR spectroscopy and X-ray crystal structure analysis (*vide infra*), cf. Fig. 5.

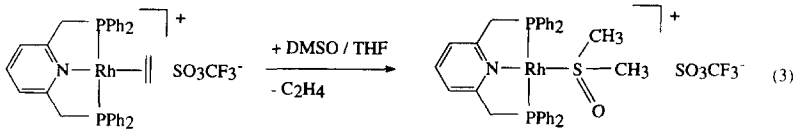

(3)

5

The complex $[Rh(PNP)(DMSO)]SO_3CF_3$ (**5**) is a yellow air stable crystalline solid. The complex was characterized by IR, ^{31}P-, ^1H-, and ^{13}C-NMR spectroscopy. In the IR spectrum of **5** the bands at 1600 and 1562 cm^{-1} indicate the coordination of the PNP pyridine ring while those of the triflate ion indicate its non-coordination as was observed for **3** and **4**. The band at 1100 cm^{-1}, assigned as $\nu(S{=}O)$, lies in the expected range for *S*-coordinated DMSO [19,20]. The ^{31}P-NMR spectrum exhibits a doublet at 36.7 ppm (J_{P-Rh} = 145 Hz). The ^1H-NMR signal of CH_3 of the coordinated DMSO at 2.68 ppm is shifted down field in comparison with the free molecule (2.49 ppm) as but not so far as it is expected for an *S*-bonded mode of DMSO [19].

X-ray quality single crystals were obtained from a solution of the complex in acetone overlayered with diethyl ether. The molecular structure of the complex cation of **5** is shown in Fig. 5. The Rh–S distance (2.1873(10) Å) is comparable to the Ru–S distance (2.188(3) Å) found in the Ru(II) complex $[Ru(NH_3)_3(DMSO)][PF_6]_2$ [21] which was described as particularly short. This may be an indication of a partial double bond character arising from d_π–p_π back donation from the metal to the sulfur. However, the S–O distance (1.473(3) Å) is not lengthened but lies within the range of the average bond length of *S*-coordinated sulfoxides [20].

Structural influences of L on the $[Rh(PNP)]^+$ fragment

In both ^{31}P NMR spectroscopy and the solid state structure, as determind by X-ray crystallography, of complexes of the type $[Rh(PNP)L]^+$ (L = Cl, py, CH_3CN, DMSO, olefin amine) the influence of different ligands on the Rh–P (*cis*) and Rh–N (*trans*) could be seen.

In Table 3 the ^{31}P-NMR results of the new cationic monoligand complexes **3–5** are assembled together with those of the chloro-, olefin, and amine PNP–rhodium(I) complexes. These are arranged in order of decreasing phosphorus–rhodium coupling constant J_{P-Rh}. Although in general the *cis* influence of a ligand is expected to be relatively small compared to its *trans* influence [22, 23] and the coupling constant J_{P-Rh} reflects only one aspect of the phosphorus–rhodium bond (primarily the s-orbital contribution to the bond order) the principal trend concerning the donor/acceptor strength can be seen in this series of the ligands. While for the σ-donor ligands (amines, chloride, and pyridine) relatively high values of J_{P-Rh} between 149 and 157 Hz were observed the phosphorus–rhodium coupling constant decreases with the increasing π-acceptor strength of the other ligands in the order: $DMSO \approx CH_3CN < C_2H_4 <$ styrene.

The influence of the negative charge of the chloro ligand can be seen in the significant up field shift to

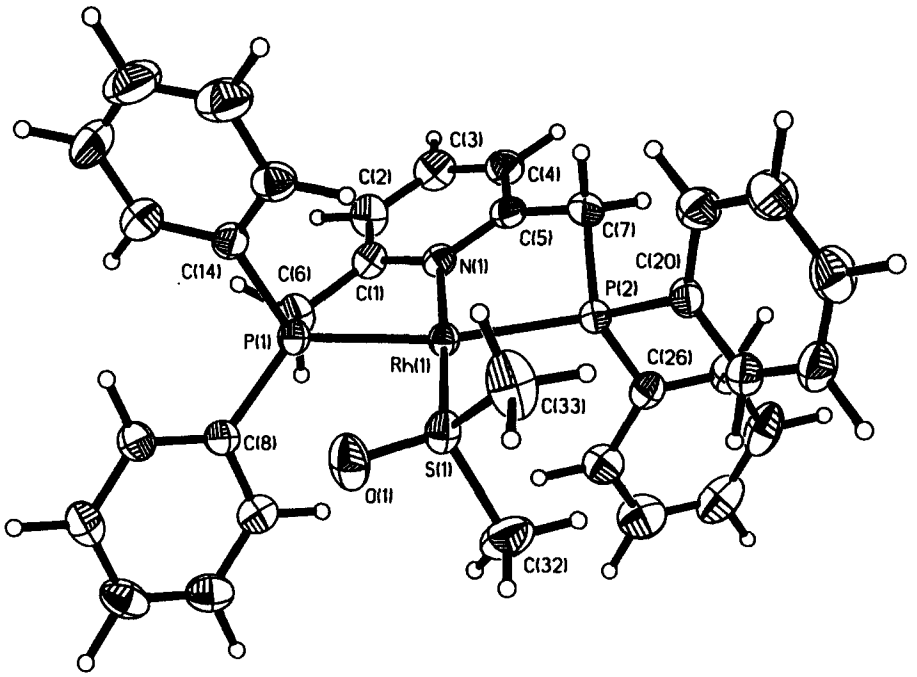

Fig. 5. ORTEP drawing structure of the cation of $[Rh(PNP)(DMSO)]SO_3CF_3 \cdot \frac{1}{2}(CH_3)_2CO$ **3**. Selected bond lengths [Å] and angles [°]: Rh—N(1) 2.093(2), Rh—S(1) 2.1870(9), Rh—P(1) 2.2696(8), Rh—P(2) 2.2884(8), S(1)—O(1) 1.474(3), S(1)—C(32) 1.786(4), P(1)—C(6) 1.839(3), P(2)—C(7) 1.841(3), P(1)—Rh—P(2) 163.76(3), N(1)—Rh—P(1) 81.84(7), N(1)—Rh—P(2) 81.91(7), N(1)—Rh—S(1) 177.48(7), O(1)—S(1)—Rh 118.76(10), C(33)—S(1)—Rh(1) 113.3(2), C(32)—S(1)—C(33) 100.5(2), O(1)—S(1)—C(32) 106.4(2).

Table 3. ^{31}P–NMR data of the PNP–rhodium(I) complexes

Complex		δ ppm	J_{P-Rh}[Hz]	Solvent
$[Rh(PNP)(HNMe_2)]BF_4$	[5]	34.3	157	Acetone-d_6
$[Rh(PNP)(HNEt_2)]BF_4$	[5]	38.9	156	Acetone-d_6
[Rh(PNP)Cl]	**1**	21.4	152	Toluene-d_8
$Rh(PNP)(py)]SO_3CF_3$	**3**	30.9	152	Acetone-d_6
$[Rh(PNP)(pip)]BF_4$	**2**	34.9	149	Acetone-d_6
$[Rh(PNP)(DMSO)]$-SO_3CF_3	**5**	36.7	145	Acetone-d_6
$[Rh(PNP)(CH_3CN)]BF_4$	**4b**	30.6	143	Acetone-d_6
$[Rh(PNP)(C_2H_4)]SO_3CF_3$	[5]	38.2	131	Acetone-d_6
$[Rh(PNP)(styrene)]BF_4$	[5]	41.7	126	Acetone-d_6

21.4 ppm. This is in contrast to the cationic complexes which are all observed at a lower field than 30 ppm. Since different structural and electronic factors of the neutral ligands have to be take into consideration it is difficult to explain completely the ordering of the ^{31}P-NMR shifts of the corresponding PNP complexes. However, comparing for example the pyridine and the styrene complexes (30.9 and 41.7 ppm, resp.) the main features of their bonding character are distinguishable, the strong σ-donating of the pyridine and the strong π-accepting property of the styrene, which seem to have an unambiguous effect on the total electron density of the $[Rh(PNP)]^+$ fragment.

Further information about the extent of the influence of the ligands on the structure of the complex fragment is obtained from the X-ray crystal structures of these complexes. In each of these complexes the PNP and the respective ligand L generates a nearly square planar coordination geometry (cf. Figs 1–5). In all cases a P(1)–Rh–P(2) angle of 163° was observed (cf. Table 4) comparable to that found in the olefin complexes of 161° [5]. Presumably, the geometric strain by the two five-membered rings formed by the coordination of the chelate PNP ligand at the rhodium atom does not allow any appreciable variation of the coordination geometry in the $[Rh(PNP)]^+$ moiety.

No significant distortion of the N(1)–Rh–L angle from linearity was observed with variation of the ligand L ranging from 178.10(12)° (Cl) to 175.55(14)° (pip). It is to be noted that in rhodium(I) complexes of the analogous type [Rh(ttp)(L)]X with the tridentate triphosphine ligand $PhP(CH_2CH_2CH_2PPh_2)_2$ (ttp), which forms two six-membered rings in the chelate structure, significant *trans* influence and steric distortion effects of a series of σ-donor and π-acceptor ligands L were distinguishable [24].

While the influence of the ligands L on the distortion from the planar coordination geometry is not pronounced in the Rh(PNP) complexes an influence

Table 4. Structural data of the X-ray crystal structure analyses of [Rh(PNP)Cl] and [Rh(PNP)L]X complexes (X = BF_4, SO_3CF_3)

Complex	Rh—N(1)	Rh—P(1) Rh—P(2)	Rh—L	N(1)—Rh—L	P(1)—Rh—P(2)
[Rh(PNP)Cl]	2.040(4)	2.263(2) 2.260(13)	2.344(2)	178.10(12)	163.53(5)
[Rh(PNP)(pip)]BF_4	2.062(3)	2.2512(10) 2.3051(10)	2.1212(3)	175.57(12)	163.43(4)
[Rh(PNP)(py)]SO_3CF_3	2.068(4)	2.2705(12) 2.2819(13)	2.063(4)	177.37(14)	163.06(4)
[Rh(PNP)(CH_3CN)]BF_4	2.045(3)	2.2648(8) 2.2770(8)	1.9884(3)	175.53(14)	166.34(4)
[Rh(PNP)(DMSO)]SO_3CF_3	2.093(2)	2.2696(8) 2.2884(8)	2.1873(10)	177.48(7)	163.76(3)
[Rh(PNP)(C_2H_4)]BF_4	2.092(4)	2.2690(13) 2.3001(13)	Rh—C(32) 2.142(6) Rh—C(33) 2.157(6)	N—Rh—C(32) 156.3(3) N—Rh—C(33) 166.8(2)	161.39(5)
[Rh(PNP)(styrene)]BF_4	2.102(3)	2.2916(10) 2.3004(11)	Rh—C(32) 2.144(5) Rh—C(33) 2.201(4)	N—Rh—C(32) 157.0(2) N—Rh—C(33) 165.8(2)	161.96(4)

on the Rh–N(1) and Rh–P bond length could be detected. An examination of the Rh–P bond length shows that in complexes bearing more bulky ligands such as piperidine or DMSO the bond length are significantly different. This feature is also found in the PEt_3 complex [Rh(ttp)(PEt_3)]AsF_6 [24] caused by intramolecular interaction between the ligand moiety and the phenyl rings of the diphenylphosphino groups.

However, on the ^{31}P-NMR time scale in each case the both phosphorus atoms of the PNP complexes are equivalent, and comparing the ordering of $J_{P\text{-}Rh}$ to the average of the Rh–P(1) and Rh–P(2) distances (2.261 Å Cl, 2.271 Å CH_3CN, 2.276 Å py, 2.278 Å pip, 2.279 Å DMSO, 2.284 Å C_2H_4, 2.296 Å styrene) a good agreement exists, reflecting the expected *cis* influence of the ligands.

The order of increasing Rh–N(1) bond length is also consistent with the expected strength of the *trans* influence of these ligands. The shortest Rh–N(1) bond length (2.040 Å), is found in the case of Cl^-, the σ-donor ligand with the highest electronegativity. On the other hand significant Rh–N(1) bond lengthening occurs with the *S*- and *C*-ligands with the lowest electro-negativity: 2.092 Å for DMSO, 2.092 Å for C_2H_4, and 2.102 Å for styrene. In general, however, the *trans* influence of these ligands observed in the Rh(PNP) complexes is scarcely larger than the *cis* influence.

CONCLUSION

In a manner analogous to the secondary amines it was shown that also the *N*-donor ligands pyridine and acetonitrile and the DMSO, as an *S*-donor ligand, can liberate the ethylene from [Rh(PNP)(C_2H_4)]X by the formation of the respective ligand complexes [Rh(PNP)L]X (L = py, CH_3CN, DMSO) which were fully characterized by ^{1}H-, ^{13}C-, and ^{31}P-NMR spectroscopy. On the other hand HMPT, DMF, THF and acetone are not able to displace the ethylene, indicating the weak affinity of the $[Rh(PNP)]^+$ fragment toward *O*-donor molecules. The results of the ^{31}P-NMR spectroscopy and X-ray crystal structure analyses of the chloro, amine, and olefin complexes allowed a *cis* and *trans* influence series to be established. The order Cl ≈ piperidine ≈ py < DMSO–CH_3CN < C_2H_4 < styrene observed from $J_{P\text{-}Rh}$ and the average Rh–P bond lengths in the Rh(PNP) complexes characterizing the *cis* influence is in good agreement with that of the *trans* influence on the Rh–N(1) bond length which is slightly pronounced. Both *cis* and *trans* influence of these ligands are obviously consistent with in general the expected order concerning their electronegativity. However, the $[Rh(PNP)]^+$ fragment must be characterized as a rigid complex moiety which is rather insensitive toward a variety of ligands.

Since the formation and the cleavage of a Rh–C σ-bond play an essential role in the catalytic cycle of the hydroamination of ethylene it is of interest to investigate its nature in the related organo–PNP–rhodium(I) complexes, which we have already prepared as further model compounds in this complex series which will be reported in another paper.

Acknowledgements—We thank the Deutsche Forschungsgemeinschaft (Sonderforschungsbereich 347 of the University Würzburg) for financial support.

REFERENCES

1. (a) Taube, R., in *Applied Homogeneous Catalysis with Organometallic Compounds*, Vol. 1, ed. B. Cornils and W. A. Herrmann. Verlag Chemie, Weinheim, 1996, pp. 507; (b) Steinborn, D. and Taube, R., *Z. Chem.*, 1986, **26,** 349; (c) Brunet, J.-J., Neibecker, D. and Niedercorn, F. J., *J. Mol. Catal.*, 1989, **49,** 235; (d) Brunet, J.-J., *Gazz. Chim. Ital.*, 1997, **127,** 111.
2. Krukowka, E., Dissertation, TH Merseburg, 1985.
3. Krukowka, E., Taube, R. and Steinborn, D., DD 296 909 A5 (10.11.88) 1988, C. A. 1992, **116,** 2139936.
4. Dahlhoff, W. V. and Nelson, S. M., *J. Chem. Soc. (A)*, 1971, 2184.
5. Hahn, C., Sieler, J. and Taube, R., *Chem. Ber.*, 1997, **130,** 939.
6. Vasapollo, G., Giannoccaro, P., Nobile, C. F. and Sacco, A., *Inorg. Chim. Acta*, 1981, **48,** 125.
7. Lange, B. and Vejdelek, Z. J., *Kolorimetrische Analyse*. Verlag Chemie, 1982, p. 232.
8. v. d. Ent, A. and Onderdelinden, A. L., *Inorg. Synth.*, 1968, **14,** 92.
9. Sheldrick, G. M., SADABAS, Program for Empirical Absorption Correction, University of Göttingen, 1996.
10. Sheldrick, G. M., SHELXS-86, Program for Crystal Structure Solution, University of Göttingen, 1986.
11. Sheldrick, G. M., SHELXL-93, Program for Crystal Structure Determination, University of Göttingen, 1993.
12. Bennett, M. J. and Donaldson, P. B., *Inorg. Chem.*, 1977, **16,** 655.
13. Selent, D., Scharfenberg-Pfeiffer, D., Reck, G. and Taube, R., *J. Organomet. Chem.*, 1991, **415,** 417.
14. Aresta, M. and Quaranta, E., *Organomet.*, 1993, **12,** 2032.
15. Beck, W. and Sünkel, K., *Chem. Rev.*, 1988, **88,** 1405.
16. Storhoff, B. N. and Lewis, H. C., *Coord. Chem. Rev.*, 1977, **23,** 1.
17. Pimblettt, G., Garner, C. D. and Clegg, W., *J. Chem. Soc., Dalton Trans.*, 1985, 1977.
18. Schrock, R. R. and Osborn, J. A., *J. Am. Chem. Soc.*, 1971, **93,** 3089.
19. Davies, J. A., *Adv. Inorg. Chem. Radiochem.*, 1981, **24,** 115.
20. Calligaris, M. and Carugo, O., *Coord. Chem. Rev.*, 1996, **153,** 83.
21. March, F. C. and Ferguson, G., *Can. J. Chem.*, 1971, **49,** 3590.
22. Hartley, F. R., *Chem. Soc. Rev.*, 1973, **2,** 163.
23. Burdett, J. K. and Albright, T. A., *Inorg. Chem.*, 1979, **18,** 2112.
24. Christoph, G. G., Blum, P., Liu, W. C., Elia, A. and Meek, D. W., *Inorg. Chem.*, 1979, **18,** 894.